J|A|C|S ARTICLES

Published on Web 08/28/2009

Length Dependence for Intramolecular Energy Transfer in Three- and Four-Color Donor−Spacer−Acceptor Arrays

Anthony Harriman,*,† Laura J. Mallon,† Kristopher J. Elliot,† Alexandre Haefele,‡ Gilles Ulrich,‡ and Raymond Ziessel*,‡

Molecular Photonics Laboratory, School of Chemistry, Bedson Building, Newcastle University, Newcastle upon Tyne, NE1 7RU, United Kingdom, and Laboratoire de Chimie Organique et Spectroscopies Avancées (LCOSA), Ecole Européenne de Chimie, Polymères et Matériaux, Université de Strasbourg, 25 rue Becquerel, 67087 Strasbourg Cedex 02, France

Received May 13, 2009; E-mail: anthony.harriman@ncl.ac.uk; ziessel@unistra.fr

Abstract: A series of donor−spacer−acceptor triads has been synthesized and fully characterized. Both donor and acceptor units are built from boron dipyrromethene (BODIPY) dyes but they differ in their respective conjugation lengths, and thereby offer quite disparate optical properties. The spacer units comprise an oligomer of 1,4-phenylene-diethynylene repeat units and allow the boron−boron separation distance to be varied progressively from 18 to 38 Å. A notable feature of this series is that each subunit can be selectively excited with monochromatic light. Highly efficacious electronic energy transfer (EET) occurs from the first-excited singlet state localized on the conventional BODIPY dye to its counterpart resident on the expanded BODIPY-based nucleus, but the rate constant follows a nonlinear evolution with separation distance. Overall, the rate of EET falls by only a factor of 4-fold on moving from the shortest to the longest spacer. This shallow length dependence is a consequence of the energy gap between donor and spacer units becoming smaller as the molecular length increases. Interestingly, a simple relationship exists between the measured electronic resistance of the spacer unit and the Huang−Rhys factor determined by emission spectroscopy. Both parameters relate to the effective conjugation length. Direct illumination of the spacer unit leads to EET to both terminals, followed by EET from conventional BODIPY to the expanded version. In each case, EET to the expanded dye involves initial population of the second-singlet excited state, whereas transfer from spacer to the conventional BODIPY dye populates the S_2 state for shorter lengths but the S_1 state for the longer analogues. The rate of EET from spacer to conventional BODIPY dye, as measured for the corresponding molecular dyads, is extremely fast ($>10^{11}$ s^{-1}) and scales with the spectral overlap integral. The relative partitioning of EET from the spacer to each terminal is somewhat sensitive to the molecular length, with the propensity to populate the conventional BODIPY dye changing from 65% for $N = 0$ to 45% for $N = 2$. The most likely explanation for this behavior can be traced to the disparate spectral overlap integrals for the two dyes. These systems have been complemented by a molecular tetrad in which pyrene residues replace the fluorine atoms present on the conventional BODIPY-based dye. Here, rapid EET occurs from pyrene to the BODIPY dye and is followed by slower, long-range EET to the opposite terminal. Such materials are seen as highly attractive solar concentrators when dispersed in transparent plastic media and used under conditions where both inter- and intramolecular EET operate.

Introduction

Electronic energy transfer (EET) has been studied for more than five decades, in both natural and artificial systems, but the subject still continues to attract considerable attention.[1] Among the many diverse examples of recent investigations into the rates and mechanisms of EET have been studies carried out with molecular arrays,[2] dendrimers,[3] liquid crystals,[4] aggregates,[5] conducting polymers,[6] thin films,[7] monomolecular layers,[8] supercritical fluids,[9] nanotubes,[10] and ionic liquids.[11] Additional attention has been given to biological samples, including protein matrices,[12] carotenoids,[13] light-harvesting complexes,[14] supramolecular arrays,[15] enzymes,[16] green fluorescent proteins,[17] and DNA.[18] Two main mechanisms are usually invoked to explain EET between weakly coupled reactants, although finer

† Newcastle University.
‡ Université de Strasbourg.

(1) Cheng, Y.-C.; Fleming, G. R. *Annu. Rev. Phys. Chem.* **2009**, *60*, 241–262.

(2) (a) Hasselman, G. M.; Watson, D. F.; Stromberg, J. R.; Bocian, D. F.; Holten, D.; Lindsey, J. S.; Meyer, G. J. *J. Phys. Chem. B* **2006**, *110*, 25430–25440. (b) Park, M.; Cho, S.; Yoon, Z. S.; Aratani, N.; Osuka, A.; Kim, D. *J. Am. Chem. Soc.* **2005**, *127*, 15201–15206. (c) Hwang, I. W.; Aratani, N.; Osuka, A.; Kim, D. *Bull. Korean Chem. Soc.* **2005**, *26*, 19–31. (d) Kobuke, Y.; Ogawa, K. *Bull. Chem. Soc. Jpn.* **2003**, *76*, 689–708. (e) Yeow, E. K. L.; Ghiggino, K. P. *J. Phys. Chem. A* **2000**, *104*, 5825–5836. (f) Benniston, A. C.; Harriman, A.; Pariani, C.; Sams, C. A. *J. Phys. Chem. A* **2007**, *111*, 8918–8924. (g) Li, F. R.; Yang, S. I.; Ciringh, Y. Z.; Seth, J.; Martin, C. H.; Singh, D. L.; Kim, D. H.; Birge, R. R.; Bocian, D. F.; Holten, D.; Lindsey, J. S. *J. Am. Chem. Soc.* **1998**, *120*, 10001–10017.

details are often necessary to account for the rates,[19] and these are loosely termed Förster-type Coulombic transfer[20] and Dexter-type electron exchange.[21] Individual studies have addressed issues such as the distance dependence,[22] temperature effects,[23] polarity changes,[24] bridge-mediated EET,[25] through-space versus through bond interactions,[26] induced switching between mechanisms,[27] concerted conformational motion,[28] quantum effects,[29] and coupled soliton involvement.[30] Numerous applications of EET have arisen, including measuring distances in biological materials,[31] improved efficacy of organic light-emitting diodes,[32] chemical sensors,[33] measuring phase transformations,[34] advanced photochromic devices,[35] and sensitized solar cells.[36] The field includes singlet−singlet, singlet−triplet,

(3) (a) Bergamini, G.; Ceroni, P.; Balzani, V.; Kandre, R.; Lukin, P. *ChemPhysChem* **2009**, *10*, 265–269. (b) D'Ambruoso, G. D.; McGrath, D. V. *Photoresponsive Polym. II* **2008**, *214*, 87–147. (c) Augulis, R.; Pugzlys, A.; Hurenkamp, J. H.; Ferringa, B. L.; van Esch, J. H.; van Loosdrecht, P. H. M. *J. Phys. Chem. A* **2007**, *111*, 12944–12953. (d) Larsen, J.; Bruggemann, B.; Khoury, T.; Sly, J.; Crossley, M. J.; Sundstrom, V.; Akesson, E. *J. Phys. Chem. A* **2007**, *111*, 10589–10597.

(4) (a) Li, X. Q.; Zhang, X.; Ghosh, S.; Wurther, F. *Chem.—Eur. J.* **2008**, *14*, 8074–8078. (b) Tcherniak, A.; Solis, D.; Khatua, S.; Tangonan, A. A.; Lee, T. R.; Link, S. *J. Am. Chem. Soc.* **2008**, *130*, 12262–12263. (c) Camerel, F.; Bonardi, L.; Ulrich, G.; Charbonniere, L.; Donnio, B.; Bourgogne, C.; Guillon, D.; Retailleau, P.; Ziessel, R. *Chem. Mater.* **2006**, *21*, 5009–5021. (d) Bobrovsky, A.; Shibaev, V.; Wendorff, J. *Liq. Cryst.* **2006**, *33*, 907–912.

(5) (a) Rolinski, O. J.; Birch, D. J. S. *J. Chem. Phys.* **2008**, *129*, 144507/1–144507/7. (b) Flamigni, L.; Ventura, B.; Oliva, A. L.; Ballester, P. *Chem.—Eur. J.* **2008**, *14*, 4214–4224. (c) Roger, C.; Miloslavina, Y.; Brunner, D.; Holzwarth, A. R.; Wurther, F. *J. Am. Chem. Soc.* **2008**, *130*, 5929–5939. (d) Kobayashi, T.; Taneichi, T.; Takasaka, S. *J. Chem. Phys.* **2007**, *126*, 194705/1–194705/4.

(6) (a) Schwartz, B. J. *Annu. Rev. Phys. Chem.* **2003**, *54*, 141–172. (b) Pei, J.; Liu, X. L.; Yu, W. L.; Lai, Y. H.; Niu, Y. H.; Cao, Y. *Macromolecules* **2002**, *35*, 7274–7280. (c) Padmanaban, G.; Ramakrishnan, S. *J. Am. Chem. Soc.* **2000**, *122*, 2244–2251. (d) Jiang, B. W.; Yang, S. W.; Bailey, S. L.; Hermans, L. G.; Niver, R. A.; Bolcar, M. A.; Jones, W. E. *Coord. Chem. Rev.* **1998**, *171*, 365–386.

(7) (a) Shaw, P. E.; Ruseckas, A.; Samuel, I. D. W. *Phys. Rev. B* **2008**, *78*, 245201/1–245201/5. (b) Dovgolevsky, E.; Kirmayer, S.; Lakin, E.; Yang, Y.; Brinker, C. J.; Frey, G. L. *J. Mater. Chem.* **2008**, *18*, 423–436. (c) Czimerova, A.; Iyi, N.; Bujdak, J. *J. Colloid. Interfac. Sci.* **2007**, *306*, 316–322. (d) Farinha, J. P. S.; Spiro, J. G.; Winnik, M. A. *J. Phys. Chem. B* **2004**, *108*, 16392–16400.

(8) (a) Kaunisto, K.; Chukharev, V.; Tkachenko, N. V.; Efimov, A.; Lemmetyinen, H. *J. Phys. Chem. C* **2009**, *113*, 3819–3825. (b) Ibrayev, N. *Russ. Phys. J.* **2008**, *51*, 725–729. (c) Cole, A.; Jana, N. R.; Selvan, S. T.; Ying, J. T. *Langmuir* **2008**, *24*, 8181–8186. (d) Lehtivuori, H.; Lemmetyinen, H.; Tkachenko, N. V. *J. Am. Chem. Soc.* **2006**, *128*, 16036–16037.

(9) (a) Zhang, J. W.; Roek, D. P.; Chateauneuf, J. E.; Brennecke, J. F. *J. Am. Chem. Soc.* **1997**, *119*, 9980–9991. (b) Bai, H.; Li, C.; Shi, G. Q. *Sens. Actuators, B* **2008**, *130*, 777–782.

(10) (a) Wong, C. Y.; Curutchet, C.; Tretiak, S.; Scholes, G. D. *J. Chem. Phys.* **2009**, *130*, 081104/1−081104/4. (b) Vlaming, S. M.; Augulis, R.; Stuart, M. C. A.; Knoester, J.; Loosdrecht, P. H. M. *J. Phys. Chem. B* **2009**, *113*, 2273–2283. (c) Swathi, R. S.; Sebastian, K. L. *J. Chem. Phys.* **2008**, *129*, 054703/1−054703/9. (d) Abe, K.; Kosumi, D.; Yanagi, K.; Miyata, Y.; Kataura, H.; Yoshizawa, M. *Phys. Rev. B* **2008**, *77*, 165436/1–165436/6.

(11) Gardinier, W. E.; Baker, G. A.; Baker, S. N.; Bright, F. V. *Macromolecules* **2005**, *38*, 8574–8582.

(12) (a) Takeda, S.; Kamiya, N.; Arai, R.; Nagamune, T. *Biochem. Biophys. Res. Commun.* **2001**, *289*, 299–304. (b) Strambini, G. B.; Gabellierie, E. *J. Phys. Chem.* **1991**, *95*, 4347–4352.

(13) (a) Balashov, S. P.; Imasheva, E. S.; Wang, J. M.; Lanyi, J. K. *Biophys. J.* **2008**, *95*, 2402–2414. (b) Polivka, T.; Pascher, T.; Hiller, R. G. *Biophys. J.* **2008**, *94*, 3198–3207. (c) Lin, S.; Katilius, E.; Ilagan, R. P.; Gibson, G. N.; Frank, H. A.; Woodbury, N. W. *J. Phys. Chem. B* **2006**, *110*, 15556–15563. (d) You, Z. Q.; Hsu, C. P.; Fleming, G. R. *J. Chem. Phys.* **2006**, *124*, 044506/1−044506/10.

(14) (a) Linnanto, J. M.; Korppi-Tommola, J. E. I. *Chem. Phys.* **2009**, *357*, 171–180. (b) Nagata, N.; Kuramouchi, Y.; Kobuke, Y. *J. Am. Chem. Soc.* **2009**, *131*, 10–15. (c) Vassiliev, S.; Bruce, D. *Photosynth. Res.* **2008**, *97*, 75–89. (d) Endo, M.; Fujitsuka, M.; Majima, T. *Chem.—Eur. J.* **2007**, *13*, 8660–8666.

(15) (a) Huang, C. H.; Bassani, D. M. *Eur. J. Org. Chem.* **2005**, 4041–4050. (b) Ajayaghosh, A.; Praveen, V. K.; Vilayakumar, C. *Chem. Soc. Rev.* **2008**, *37*, 109–122. (c) Zhang, H.; Hoeben, F. J. M.; Pouderoijen, M. J.; Schenning, A. P. H. L.; Meijer, E. J.; De Schryver, F. C.; De Feyter, S. *Chem.—Eur. J.* **2006**, *12*, 9046–9055.

(16) (a) Zheng, X. H.; Garcia, J.; Stuchebrukhov, A. A. *J. Phys. Chem. B* **2008**, *112*, 8724–8729. (b) Chandrakuntal, K.; Thomas, N. M.; Kumar, P. G.; Laloraya, M.; Laloraya, M. M *Photochem. Photobiol.* **2006**, *82*, 1358–1364. (c) Kuznetsova, S.; Zauner, G.; Schmauder, R.; Maybroroda, O. A.; Deelder, A. M.; Aartsma, T. J.; Canters, G. W. *Anal. Biochem.* **2006**, *350*, 52–60. (d) Henry, A. A.; Jimenez, R.; Hanway, D.; Romerberg, F. E. *ChemBioChem* **2004**, *5*, 1088–1094.

(17) (a) Wang, Y. X.; Shyy, J. Y. J.; Chien, S. *Annu. Rev. Biomed. Eng.* **2008**, *10*, 1–38. (b) Dinant, C.; van Royen, M. E.; Vermeulen, W.; Houtsmuller, A. B. *J. Microsc.* **2008**, *231*, 97–104.

(18) (a) Hannestad, J. K.; Sandin, P.; Albinsson, B. *J. Am. Chem. Soc.* **2008**, *130*, 15889–15895. (b) Hurley, D. J.; Tor, Y. *J. Am. Chem. Soc.* **2002**, *124*, 13231–13241. (c) Holmlin, R. E.; Tong, R. T.; Barton, J. K. *J. Am. Chem. Soc.* **1998**, *120*, 9724–9725. (d) Brun, A. M.; Harriman, A. *J. Am. Chem. Soc.* **1994**, *116*, 10383–10393.

(19) (a) Berera, R.; van Stokkum, I. H. M.; Kodis, G.; Keirstead, A. E.; Pillai, S.; Herrero, C.; Palacios, R. E.; Bengris, M.; van Grondelle, R.; Gust, D.; Moore, T. A.; Moore, A. L.; Kennis, J. T. M. *J. Phys. Chem. B* **2007**, *111*, 6868–6877. (b) Benniston, A. C.; Harriman, A.; Li, P. Y.; Patel, P. V.; Sams, C. A. *Chem.—Eur. J.* **2008**, *14*, 1710–1717.

(20) Valeur, B. *Modern Fluorescence: Principles and Applications*, Wiley-VCH: Weinheim, 2002.

(21) Anslyn, E. V.; Dougherty, D. A. *Modern Physical Organic Chemistry*; University Science Books: Sausalito, 2006.

(22) (a) Harriman, A.; Khatyr, A.; Ziessel, R.; Benniston, A. C. *Angew. Chem., Int. Ed.* **2000**, *39*, 4287–4290. (b) Albinsson, B.; Martensson, J. *J. Photochem. Photobiol., C* **2008**, *9*, 138–155. (c) Schrier, J.; Wang, L. W. *J. Phys. Chem. C* **2008**, *112*, 11158–11161. (d) Romanova, Z. S.; Deshayes, K.; Piotrowiak, P. *J. Am. Chem. Soc.* **2001**, *123*, 11029–11036.

(23) (a) Benniston, A. C.; Harriman, A.; Li, P. Y.; Sams, C. A. *J. Am. Chem. Soc.* **2005**, *127*, 2553–2564. (b) Piston, D. W.; Kremers, G. J. *Trends Biochem. Sci.* **2007**, *32*, 407–414. (c) Perham, M.; Wittung-Stafshede, P. *Arch. Biochem. Biophys.* **2007**, *464*, 306–313. (d) Robinson, J. M.; Dong, W. J.; Cheung, H. C. *J. Mol. Biol.* **2003**, *329*, 371–380.

(24) (a) Shanks, D.; Preus, S.; Qvortrup, K.; Hassenkam, T.; Nielsen, M. B.; Kilsa, K. *New J. Chem.* **2009**, *33*, 507–516. (b) Tannert, S.; Ermilov, E. A.; Vogel, J. O.; Choi, M. T. M.; Ng, D. K. P.; Roeder, B. *J. Phys. Chem. B* **2007**, *111*, 8053–8062.

(25) (a) Chen, H. C.; You, Z. Q.; Hsu, C. P. *J. Chem. Phys.* **2008**, *129*, 084708/1−084708/10. (b) May, V. *J. Chem. Phys.* **2008**, *129*, 114109/1–114109/15. (c) Fueckel, B.; Koehn, A.; Harding, M. E.; Diezemann, G.; Hinze, G.; Basche, T.; Gauss, J. *J. Chem. Phys.* **2008**, *128*, 074505/1−074505/13. (d) Lokan, N. R.; Paddon-Row, M. N.; Koeberg, M.; Verhoeven, J. W. *J. Am. Chem. Soc.* **2000**, *122*, 5075–5081.

(26) (a) Kelley, R. F.; Lee, S. J.; Wilson, T. M.; Nakamura, Y.; Tiede, D. M.; Suka, A.; Hupp, J. T.; Wasielewski, M. R. *J. Am. Chem. Soc.* **2008**, *130*, 4277–4284. (b) Van Averbeke, B.; Beljonne, D.; Hennebicq, E. *Adv. Funct. Mater.* **2008**, *18*, 492–498. (c) Allen, B. D.; Benniston, A. C.; Harriman, A.; Mallon, L. J.; Pariani, C. *Phys. Chem. Chem. Phys.* **2006**, *8*, 4112–4118. (d) Song, H. E.; Kirmaier, C.; Schwartz, J. K.; Hindin, E.; Yu, L. H.; Bocian, D. F.; Lindsey, J. S.; Holten, D. *J. Phys. Chem. B* **2006**, *110*, 19121–19130.

(27) (a) Andrews, D. L. *Can. J. Chem.* **2008**, *86*, 855–870. (b) Lammi, R. K.; Wagner, R. W.; Ambroise, A.; Diers, J. D.; Bocian, D. F.; Holten, D.; Lindsey, J. S. *J. Phys. Chem. B* **2001**, *105*, 5341–5352. (c) Grosshenny, V.; Harriman, A.; Hissler, M.; Ziessel, R. *J. Chem. Soc., Faraday Trans.* **1996**, *92*, 2223–2238.

(28) (a) Van Averbeke, B.; Beljonne, D. *J. Phys. Chem. A* **2009**, *113*, 2677–2682. (b) Vasquez, S. O. *Phys. Chem. Chem. Phys.* **2008**, *10*, 5459–5468. (c) Zurn, A.; Zabel, U.; Vilardaga, J. P.; Schindelin, H.; Lohse, M. J.; Hoffmann, C. *Mol. Phamacol.* **2009**, *75*, 534–541. (d) Du, M.; Rambhadran, A.; Jayaraman, V. *J. Biol. Chem.* **2008**, *283*, 27074–27078.

(29) Olaya-Castro, A.; Lee, C. F.; Olsen, F. F.; Johnson, N. F. *Phys. Rev. B* **2008**, *78*, 085115/1−085115/7.

(30) (a) de Jonge, J. J.; Ratner, M. A.; de Leeuw, S. W.; Simonis, R. O. *J. Phys. Chem. B* **2004**, *108*, 2666–2675. (b) Falvo, C.; Pouthier, V.; Eilbeck, J. C. *Physica D* **2006**, *221*, 58–71. (c) Brizhik, L.; Eremko, A.; Piette, B.; Zakrze, W. *Chem. Phys.* **2006**, *324*, 259–266. (d) Hennig, D. *Eur. Phys.J. B* **2001**, *24*, 377–381.

triplet−triplet, and triplet−multiplet processes, covering liquid, solid, and gaseous samples. Other research combines EET with subsequent electron-transfer reactions, often under the general heading of artificial photosynthesis.[37] Recent advances in the EET field have been reviewed.[38]

Numerous contemporary publications have been concerned with EET in molecular assembles built around boron dipyrromethene (BODIPY) dyes.[39] This work includes closely spaced dyads with the BODIPY dye acting as acceptor,[40] linear triads,[41] molecular dyads constructed from different types of BODIPY dyes,[42] BODIPY dyes attached to metal complexes,[43] EET in crystals and other organized media,[44] and multichromophoric arrays.[45] Such studies are assisted by the intense fluorescence inherent to the basic BODIPY framework, the versatile synthetic protocols applicable to this class of dye, the favorable photophysical properties (e.g., narrow absorption and emission spectral profiles), and the absence of significant medium effects.[39] Many of these studies have focused on mechanistic aspects of the EET process. We now extend this work by examining EET in a series of BODIPY-based triads where the terminals are two optically distinct BODIPY dyes and the spacers are poly(aryl) units of differing length; it should be noted that several examples of symmetrical triads have appeared of late, having identical BODIPY units attached at either end of a short poly(aryl) spacer.[46] As well as monitoring how the rate of EET evolves with increasing molecular length, the new series allows critical comparison of the fate of photons absorbed directly by the spacer (Scheme 1). Thus, the singlet-excited state of the terminal BODIPY donor can participate in long-range EET to the opposite end of the molecule, this process being driven by a reasonably large energy gap. The corresponding singlet-excited state formed upon direct light absorption by the spacer can undergo EET to either terminal, and an important objective is to establish the partition function for such behavior. Three-color triads of this type are rare, and little attention has been given to understanding the energy-transfer dynamics in

(31) (a) O'Brien, E. P.; Morrison, G.; Brooks, B. R.; Thirumalai, D. *J. Chem. Phys.* **2009**, *130*, 124903/1–124903/10. (b) Vamosi, G.; Clegg, R. A. *J. Phys. Chem. B* **2008**, *112*, 13136–13148. (c) Nettels, D.; Hoffmann, A.; Schuler, B. *J. Phys. Chem. B* **2008**, *112*, 6137–6146. (d) Chowdhury, R. P.; Chatterjee, D. *Biophys. Chem.* **2007**, *128*, 19–29.

(32) (a) Bugar, I.; Zitnan, M.; Velic, D.; Cik, G.; Chorvat, D. *Synth. Met.* **2007**, *157*, 834–840. (b) Gupta, D.; Katiyar, M.; Deepak, D.; Hazra, T.; Marloharan, S. S.; Biswas, A. *Opt. Mater.* **2006**, *28*, 1355–1361. (c) Hepp, A.; Ulrich, G.; Schmechel, R.; Ziessel, R. *Synth. Met.* **2004**, *146*, 11–15. (d) Kim, J. S.; Seo, B. W.; Gu, H. B. *Synth. Met.* **2003**, *132*, 285–288.

(33) (a) McDonagh, C.; Burke, C. S.; MacCraith, B. D. *Chem. Rev.* **2008**, *108*, 400–422. (b) Fan, F. J.; Zhang, Y.; Murphy, C. B.; Angell, S. E.; Parker, M. F. L.; Flynn, B. R.; Jones, W. E. *Coord. Chem. Rev.* **2009**, *253*, 410–422. (c) Borisov, S. M.; Wolfbeis, O. S. *Chem. Rev.* **2008**, *108*, 423–461. (d) Sapsford, K. E.; Bradburne, C.; Detehanty, J. B.; Medintz, I. L. *Mater. Today* **2008**, *11*, 38–49.

(34) (a) Wu, C. F.; McNeill, J. *Langmuir* **2008**, *24*, 5855–5861. (b) Bacchiocchi, C.; Zannoni, C. *Chem. Phys. Lett.* **1997**, *268*, 541–548. (c) Fonteijn, T. A. A.; Engberts, J. B. F. N.; Hoekstrad, D. *Biochem.* **1991**, *30*, 5319–5324.

(35) (a) Jukes, R. T. F.; Bozic, B.; Belser, P.; De Cola, L.; Hartl, F. *Inorg. Chem.* **2009**, *48*, 1711–1721. (b) Tian, H.; Feng, Y. L. *J. Mater. Chem.* **2008**, *18*, 1617–1622. (c) Hurenkamp, J. H.; de Jong, J. J. D.; Browne, W. R.; van Esch, J. H.; Feringa, B. L. *Org. Biomol. Chem.* **2008**, *6*, 1268–1277. (d) Davis, D.; Tamaoki, N. *Chem.−Eur. J.* **2007**, *13*, 626–631. (e) Benniston, A. C.; Harriman, A.; Howell, S. L.; Li, P. Y.; Lydon, D. P. *J. Org. Chem.* **2007**, *72*, 888–897. (f) Belfield, K. D.; Bondar, M. V.; Corredor, C. C.; Hernandez, F. E.; Przhonska, O. V.; Yao, S. *ChemPhysChem* **2006**, *7*, 2514–2519.

(36) (a) Lin, C. Y.; Lo, C. F.; Luo, L.; Lu, H. P.; Hung, C. S.; Diau, E. W. G. *J. Phys. Chem. C* **2009**, *113*, 755–764. (b) Kamat, P. V. *J. Phys. Chem. C* **2008**, *112*, 18737–18753. (c) Holzhey, A.; Uhrich, C.; Brier, E.; Reinhold, E.; Bauerle, P.; Leo, K.; Hoffmann, M. *J. Appl. Phys.* **2008**, *104*, 064510/1−064510/8. (d) Siegers, C.; Hohl-Ebinger, J.; Zimmermann, B.; Wufel, U.; Mulhaupt, R.; Hinsch, A.; Haag, R. *ChemPhysChem* **2007**, *8*, 1548–1556. (e) Koeppe, R.; Bossart, O.; Calzaferri, G.; Sariciftci, N. S. *Sol. Energy Mater. Sol. Cells* **2007**, *91*, 986–995. (f) Kong, F. T.; Dai, S. Y. *Prog. Chem.* **2006**, *18*, 1409–1424.

(37) Benniston, A. C.; Harriman, A. *Mater. Today* **2008**, *11*, 26–34.

(38) (a) Bohr, H.; Greisen, P.; Malic, B. *Condens. Matter Theory* **2009**, *23*, 329–338. (b) Martinez, T. J. *Acc. Chem. Res.* **2006**, *39*, 119–126. (c) Kim, D.; Osuka, A. *Acc. Chem. Res.* **2004**, *37*, 735–745. (d) Dewey, T. G. *Acc. Chem. Res.* **1992**, *25*, 195–200. (e) Speiser, S. *Chem. Rev.* **1996**, *96*, 1953–1976. (f) Nakamura, Y.; Aratani, N.; Osuka, A. *Chem. Soc. Rev.* **2007**, *36*, 831–845. (g) Benniston, A. C.; Harriman, A. *Chem. Soc. Rev.* **2006**, *35*, 169–179. (h) Barigelletti, F.; Flamigni, L. *Chem. Soc. Rev.* **2000**, *29*, 1–12. (i) Odobel, F.; Fortage, J. *C. R. Chim.* **2009**, *12*, 437–449.

(39) (a) Ulrich, G.; Ziessel, R.; Harriman, A. *Angew. Chem., Int. Ed.* **2008**, *47*, 1184–1201. (b) Ziessel, R.; Ulrich, G.; Harriman, A. *New J. Chem.* **2007**, *31*, 496–501. (c) Ziessel, R. *C. R. Chim.* **2007**, *10*, 622–629. (d) Loudet, A.; Burgess, K. *Chem. Rev.* **2007**, *107*, 4891–4932.

(40) (a) Barin, G.; Yilmaz, M. D.; Akkaya, E. U. *Tetrahedron Lett.* **2009**, *50*, 1738–1740. (b) Liu, J. Y.; Ermilov, E. A.; Roder, B.; Ng, D. K. P. *Chem. Commun.* **2009**, 1517–1519. (c) Camerel, F.; Ulrich, G.; Retailleau, P.; Ziessel, R. *Angew. Chem., Int. Ed.* **2008**, *46*, 8876–8880. (d) Zhang, X. L.; Xiao, Y.; Qian, X. H. *Org. Lett.* **2008**, *10*, 29–32. (e) Isaksson, M.; Hagglof, P.; Hakansson, P.; Ny, T.; Johansson, L. B. Å. *Phys. Chem. Chem. Phys.* **2007**, *9*, 3914–3922. (f) Coskun, A; Akkaya, E. U. *J. Am. Chem. Soc.* **2006**, *128*, 14474–14475. (g) Harriman, A.; Izzet, G.; Ziessel, R. *J. Am. Chem. Soc.* **2006**, *128*, 10868–10875. (h) Goze, C.; Ulrich, G.; Mallon, L. J.; Allen, B. D.; Harriman, A.; Ziessel, R. *J. Am. Chem. Soc.* **2006**, *128*, 10231–10239. (i) Yilmaz, M. D.; Bozdemir, O. A.; Akkaya, E. U. *Org. Lett.* **2006**, *8*, 2871–2873. (j) Kalinin, S.; Johansson, L. B.Å. *J. Phys. Chem. B* **2004**, *108*, 3092–9097. (k) Wan, C. W.; Burghart, A.; Chen, J.; Bergstrom, F.; Johansson, L. B. Å.; Wolford, M. F.; Kim, T. G.; Topp, M. R.; Hochstrasser, R. M.; Burgess, K. *Chem.−Eur. J.* **2003**, *9*, 4430–4441. (l) Burghart, A.; Thoresen, L. H.; Chen, J.; Burgess, K.; Bergstrom, F.; Johansson, L. B. Å *Chem. Commun.* **2000**, 2203–2204. (m) Keller, R. C. A.; Silvius, J. R.; de Kruijff, B. *Biochem. Biophys. Res. Commun.* **1995**, *207*, 508–514.

(41) (a) Alamiry, M. A. H.; Harriman, A.; Mallon, L. J.; Ulrich, G.; Ziessel, R. *Eur. J. Org. Chem.* **2008**, *277*, 4–2782. (b) Tomasulo, M.; Deniz, E.; Alvarado, R. J.; Raymo, F. M. *J. Phys. Chem. C* **2008**, *112*, 8038–8045. (c) Bailey, S. T.; Lokey, G. E.; Hanes, M. S.; Shearer, J. D. M.; McLafferty, J. B.; Beaumont, G. T.; Baseler, T. T.; Layhue, J. M.; Broussard, D. R.; Zhang, Y. Z.; Wittmershaus, B. P. *Sol. Energy Mater. Sol. Cell* **2007**, *91*, 67–75. (d) Ziessel, R.; Goze, C.; Ulrich, G.; Cesario, M.; Retailleau, P.; Harriman, A.; Rostron, J. P. *Chem.−Eur. J.* **2005**, *11*, 7366–7378. (e) Koepf, M.; Trabolsi, A.; Elhabiri, M.; Wytko, J. A.; Paul, D.; Albrecht-Gary, A. M.; Weiss, J. *Org. Lett.* **2005**, *7*, 1279–1282.

(42) (a) Harriman, A.; Mallon, L. J.; Goeb, S.; Ziessel, R. *Phys. Chem. Chem. Phys.* **2007**, *9*, 5199–5201. (b) Saki, N.; Dinc, T.; Akkaya, E. U. *Tetrahedron* **2006**, *62*, 2721–2725. (c) Tleugabulova, D.; Zhang, Z.; Brennan, J. D. *J. Phys. Chem. C* **2002**, *106*, 13133–13138. (d) Mikhalyov, I.; Bogen, S. T.; Johansson, L. B. Å. *Spectrochim. Acta, Part A* **2001**, *57*, 1839–1845. (e) Johansson, L. B. Å.; Karolin, J. *Pure Appl. Chem.* **1997**, *69*, 761–765. (f) Bröring, M.; Krüger, R.; Link, S.; Kleeberg, C.; Köhler, S.; Xie, X.; Ventura, B.; Flamigni, L. *Chem.−Eur. J.* **2008**, *14*, 2976–2983. (g) Maruschchak, D.; Kalinin, S.; Mikhalyov, I.; Gretskaya, N.; Johansson, L. B. Å. *Spectrochim. Acta, Part A* **2006**, *65*, 113–122.

(43) (a) Nastasi, F.; Puntoriero, F.; Campagna, S.; Diring, S.; Ziessel, R. *Phys. Chem. Chem. Phys.* **2008**, *10*, 3982–3986. (b) Galletta, M.; Puntoriero, F.; Campagna, S.; Chiroboli, C.; Quesada, M.; Goeb, S.; Ziessel, R. *J. Phys. Chem. A* **2006**, *110*, 4348–4358.

(44) (a) Benniston, A. C.; Copley, G.; Harriman, A.; Rewinska, D. B.; Harrington, R. W.; Clegg, W. *J. Am. Chem. Soc.* **2008**, *130*, 7174–7175. (b) Erlen-Ela, S.; Yilmaz, M. D.; Icli, B.; Dede, Y.; Icli, S.; Akkaya, E. U. *Org. Lett.* **2008**, *10*, 3299–3302.

(45) (a) Harriman, A.; Mallon, L. J.; Ziessel, R. *Chem.−Eur. J.* **2008**, *14*, 11461–11473. (b) Goeb, S.; Ziessel, R. *Tetrahedron Lett.* **2008**, *49*, 2569–2574.

(46) (a) Zrig, S.; Remy, P.; Ardrioletti, B.; Rose, E.; Asselberghs, I.; Clays, K. *J. Org. Chem.* **2008**, *73*, 1563–1566. (b) Banuelos, I.; Arbeloa, F. L.; Arbeloa, T.; Salleres, S.; Amat-Guerri, F.; Liras, M.; Arbeloa, I. L. *J. Phys. Chem. A* **2008**, *112*, 10816–10822. (c) Porrès, L.; Mongin, O.; Blanchard-Desce, M. *Tetrahedron Lett.* **2006**, *47*, 1913–1917.

Scheme 1. Pictorial Illustration of EET in the Linear Triads Described Herein, Where D, Sp and A, Respectively, Refer to Donor, Spacer and Acceptor

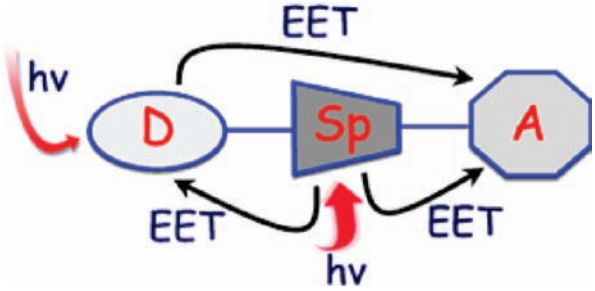

such arrays. The systems under investigation further demonstrate the versatility of the BODIPY nucleus for photophysical exploitation.

As confirmation of this latter point, one of the above molecular triads was further functionalized by replacement[47] of the B−F bonds associated with the normal BODIPY dye with pyrene residues. Although this leads to a rather congested absorption envelope in the near-UV region, it is possible to selectively illuminate into the pyrene chromophore so as to set up the possibility of a multiple cascade effect. Such systems are interesting as artificial light-harvesting units and as solar concentrators.[48] In fact, there is growing awareness of the huge potential offered by polymeric solar concentrators as a simple and economical means by which to improve the effectiveness of solar cells.[49] The new system introduced here harvests photons across most of the visible range and emits in the far-red region. An additional motivation for studying the dynamics of EET in multicomponent molecular systems stems from the growing concerns about the mechanisms of such processes in conducting polymers,[50] where Förster theory might not be appropriate to explain the long-range, coherent intrachain energy migration that has been observed in certain cases.[51] In particular, it has been stressed that there is a need to better explain EET in the intermediate coupling regime,[52] and molecules of the type described herein could be important contributors to this subject.

Results and Discussion

Synthesis. Here, we describe the photophysical properties of a series of short molecular wires bearing two different BODIPY terminals (from now on these being termed BOD and EXP, respectively, to acknowledge that the primary donor is a conventional BODIPY dye, whereas the primary acceptor has an expanded π-system) linked by 1,4-phenylene-diethynylene spacers (Figure 1). These terminals differ in their respective conjugation lengths, and hence their optical properties, and also by virtue of the site of coupling to the spacer; BOD is connected through a *meso*-phenylene ring, whereas EXP is linked to the spacer via the boron center. It should be noted that, for reasons of synthetic simplicity, the target molecules comprise a single EXP unit bearing two identical arms containing the spacer and BOD terminal. The spacers were substituted with *n*-butoxy groups in order to improve their solubility and to avoid problems caused by self-aggregation. Throughout the series of BOD_N−EXP triads, molar absorption coefficients (ε_{MAX}) measured at the peak maxima corresponded to averaged values of 69,000 and 71,000 M^{-1} cm^{-1}, respectively, for the EXP and BOD chromophores. For the spacer units present in these triads, ε_{MAX} increased progressively along the series: ε_{MAX} = 24,000 (Sp_0), 53,100 (Sp_1), 67,090 (Sp_2), and 83,750 M^{-1} cm^{-1} (Sp_3) per chromophore. Full synthetic details, and a short description of the NMR spectral features of these compounds, are given in the Supporting Information. In order to aid interpretation of the photophysical data, a series of reference compounds was also studied, and their respective molecular formulas are shown in Figure 2.

Photophysical Properties in the Absence of EET. Absorption spectra recorded for the series of molecular triads, BOD_N−EXP, in $CHCl_3$ are shown in Figure 3. The transitions localized on the individual chromophores are well resolved and easily recognized by way of reference to the model compounds. Thus, EXP absorbs intensely at wavelengths around 650 nm, whereas BOD displays a pronounced absorption envelope with a maximum at ∼530 nm. Spectra for individual members of the series are superimposable at wavelengths longer than about 490 nm, indicating the absence of significant electronic effects. In contrast, absorption spectral bands associated with the spacer unit differ markedly throughout the series, with the maximum moving progressively toward lower energy as the molecular length increases. This is a well-known effect[53] for poly(aromatics) and reflects the increased conjugation length. There is also a progressive increase in the oscillator strength for the transition as the spacer becomes longer. Again, such behavior has been reported before[54] and, for the compounds described here, serves to reduce the energy gap between singlet-excited states localized on BOD and on the spacer moiety as the series evolves. This effect has important consequences for long-range, superexchange interactions between the terminals. These spacer-based absorption transitions tend to obscure the S_0−S_2 transitions associated with the two BODIPY-based terminals, which appear in the near-UV region,[55] except for the shortest spacer. In this latter case, the onset of S_0−S_2 absorption by the terminals can be seen at around 410 nm (Figure 3). The compounds are reasonably soluble in $CHCl_3$, and there are no obvious signs of self-aggregation.

For each member of the series in dilute $CHCl_3$ solution at room temperature, excitation into the EXP unit (λ_{EXT} = 620 nm) results in fluorescence characteristic of that entity as recognized from separate studies conducted with the reference compounds. This emission is centered at ∼685 nm and retains a Stokes' shift of ∼680 cm^{-1}. The fluorescence quantum yield (Φ_F) has an average value of 0.72, identical to that measured for the reference compounds, while the average fluorescence

(47) Goze, C.; Ulrich, G.; Ziessel, R. *J. Org. Chem.* **2007**, *72*, 313–322.
(48) (a) Goldschmidt, J. C.; Peters, M.; Bosch, A.; Helmers, H.; Dimroth, F.; Glunz, S. W.; Willeke, G. *Sol. Energy Mater. Sol. Cells* **2009**, *93*, 176–182. (b) Gabr, M. *Int. J. Polym. Mater* **2008**, *57*, 569–583. (c) Ishchenko, A. A. *Pure Appl. Chem.* **2008**, 1525–1530.
(49) Slooff, L. H.; Bende, E. E.; Burgers, A. R.; Budel, T.; Pavettoni, M.; Kenny, R. P.; Dunlop, E. D.; Buchtemann, A. *Phys. Status Solidi Rapid Res. Lett.* **2008**, *2*, 257–259.
(50) Schwartz, B. J. *Annu. Rev. Phys. Chem.* **2003**, *54*, 141–172.
(51) (a) Shaw, P. E.; Ruseckas, A.; Samuel, I. D. W. *Phys. Rev. B* **2008**, *78*, 245201. (b) Rose, A.; Lugmair, C. G.; Swager, T. M. *J. Am. Chem. Soc.* **2001**, *123*, 11298–11299.
(52) Collini, E.; Scholes, G. D. *Science* **2009**, *323*, 369–373.
(53) (a) Wohlgenannt, M.; Jiang, X. M.; Vardeny, Z. V. *Phys. Rev. B* **2004**, *69*, 241204. (b) Rothe, C.; Brunner, K.; Bach, I.; Heun, S.; Monkman, A. P. *J. Chem. Phys.* **2005**, *122*, 084706/1−084706/6. (c) Casado, J.; Hick, R. G.; Hernández, V.; Myles, D. J. T.; Ruiz Delgado, M. C.; López Navarrete, J. T. *J. Chem. Phys.* **2003**, *118*, 1912–1920.
(54) Benniston, A. C.; Harriman, A.; Rewinska, D. B.; Yang, S.; Zhi, Y. G. *Chem.—Eur. J.* **2007**, *13*, 10194–10203.
(55) (a) Prieto, J. B.; Arbeloa, F. L.; Martinez, V. M.; Arbeloa, L. *Chem. Phys.* **2004**, *296*, 13–22. (b) Rurack, K.; Kollmannsberger, M.; Daub, J. *Angew. Chem., Int. Ed.* **2001**, *40*, 385–387.

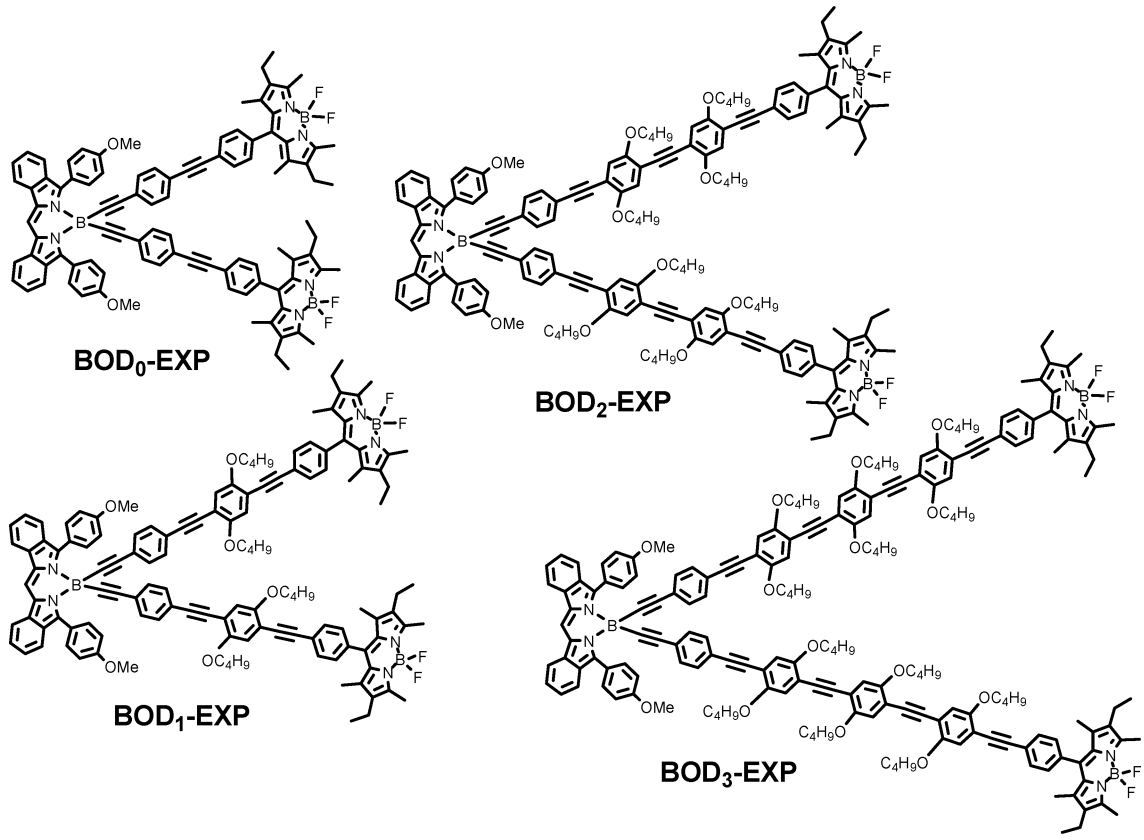

Figure 1. Molecular formulas of the target molecular triads used in this work. The numeral shown as a subscript corresponds to the number of 1-ethynyl-2,5-dibutoxyphenyl subunits in the spacer unit.

lifetime ($\tau_S = 7.9$ ns) is also the same as those found for the model dyes (Table 1). In each case, the time-resolved fluorescence decay profiles could be analyzed satisfactorily in terms of single-exponential processes. For these EXP-based fluorophores, the radiative rate constant ($k_{RAD} = 9 \times 10^7$ s^{-1}) is slightly smaller than that found for conventional BODIPY dyes, but this disparity can be attributed to the lower energy of the optical transition.[56] There are no noticeable effects of spacer length and no obvious perturbation of the photophysics by the presence of the BOD terminal. Similar conclusions are reached from spectroscopic studies carried out in methyltetrahydrofuran (MTHF) at 77 K and in a few other organic solvents at room temperature. Deconstruction of the emission spectral profiles into the minimum number of Gaussian-shaped components indicates that nonradiative decay is promoted by a medium-frequency vibronic mode ($h\omega_M = 1395$ cm^{-1}) and, in the glassy matrix, by an additional low-frequency mode ($h\omega_L = 545$ cm^{-1}) (Table 1). In all cases, the S_1 level associated with the EXP unit is located at 15,080 cm^{-1} (i.e., 1.87 eV).

Fluorescence spectra were recorded for each of the conventional BODIPY-based dyes covalently linked to a spacer moiety of differing length, BOD_N, following excitation into the dye at 510 nm. The emission maximum occurred at 545 nm in each case, while the Stokes' shift was ~560 cm^{-1}. Fluorescence quantum yields were close to unity but somewhat dependent on the length of the spacer unit, with longer spacers giving the higher Φ_F (Table 1). In contrast, the fluorescence lifetimes were found to decrease progressively with increasing length of the attached spacer unit (Table 1); in each case, the fluorescence decay profiles recorded by time-correlated, single-photon counting methods could be analyzed satisfactorily in terms of a single-exponential fit. Such properties result in the radiative rate constant (k_{RAD}) showing a modest increase with increasing number of repeat unit in the spacer, whereas the corresponding nonradiative rate constant (k_{NR}) evolves in the opposite direction. These effects are modest, however, and do not cause major perturbations of the photophysical properties of the BODIPY dye. Even so, it appears that there is a small amount of interaction between excited states localized on the two units. At 77 K in MTHF, fluorescence from the BODIPY-based dye exhibits a small blue shift and a sharpening of the spectral profile. Under these conditions, nonradiative decay of the S_1 state is promoted by coupling to a low-frequency vibronic mode of ~425 cm^{-1}. It is perhaps pertinent to note that the corresponding medium-frequency vibronic mode coupled to excited-state deactivation appears to be sensitive to the length of the bridge and increases from 1265 cm^{-1} for the shortest analogue to 1400 cm^{-1} for the longest spacer (Table 1). Direct excitation into the spacer units leads to intense fluorescence from the BODIPY-based dye at both 295 and 77 K. Under such conditions, there is little, or no, emission that could be attributed to the spacer unit itself. Corrected excitation spectra recorded for the entire series of BOD_N dyads agree very well with the corresponding absorption spectra over the range from 520 to 260 nm. Such behavior is highly indicative of efficacious intramolecular EET from spacer to dye. Indeed, on the basis of quantum yield measurements it can be concluded that the probability of EET exceeds 99% in each case.

(56) (a) Verhoeven, J. W.; Scherer, T.; Wegewijs, B.; Hermant, R. M.; Jortner, J.; Bixon, M.; Depaemelaere, S.; De Schryver, F. C. *Recl. Trav. Chim. Pays-Bas* **1995**, *114*, 443–451. (b) Bixon, M.; Jortner, J.; Verhoeven, J. W. *J. Am. Chem. Soc.* **1994**, *116*, 7349–7355.

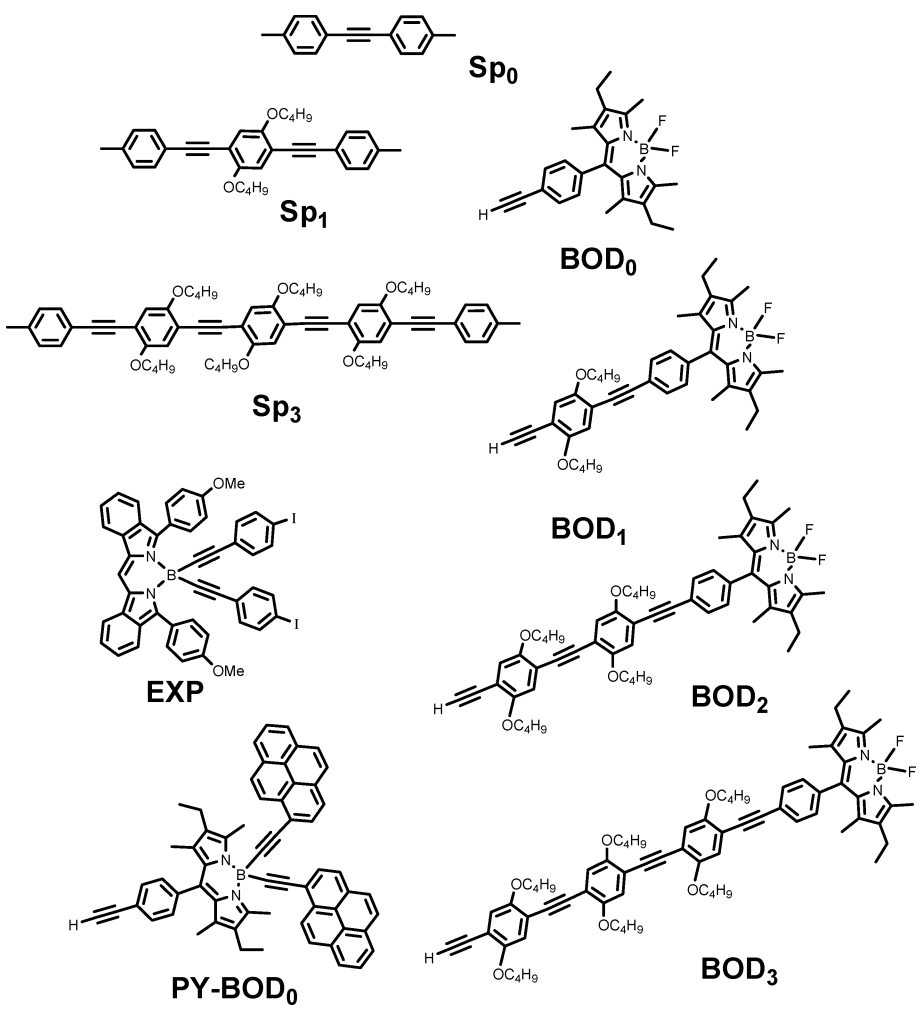

Figure 2. Molecular formulas for the various precursors and the spacers used throughout this study.

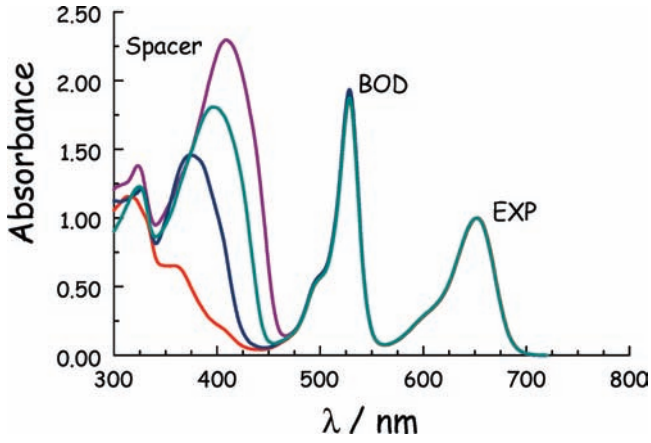

Figure 3. Absorption spectra recorded for the molecular triads in $CHCl_3$ solution at room temperature; BOD_0−EXP (red), BOD_1−EXP (dark blue), BOD_2−EXP (light blue), and BOD_3−EXP (turquoise).

Table 1. Photophysical Properties of the Various Compounds As Measured in $CHCl_3$ Solution at Room Temperature[a]

cmpd	λ_{ABS}/nm	λ_{FLU}/nm	Φ_F	τ_S/ns	SS/cm^{-1}	hω_L/cm^{-1}	hω_M/cm^{-1}
EXP	658	692	0.73	7.1	745	550	1400
BOD_0−EXP	652	684[b]	0.72	8.1	720	540	1395
BOD_1−EXP	652	682[b]	0.74	8.2	675	520	1390
BOD_2−EXP	652	682[b]	0.74	8.5	675	520	1400
BOD_3−EXP	652	684[b]	0.70	7.2	720	495	1395
BOD_0	528	544[c]	0.79	5.4	560	400	1265
BOD_1	528	544[c]	0.84	4.1	560	430	1355
BOD_2	528	544[c]	0.87	4.2	560	435	1350
BOD_3	528	544[c]	0.89	3.7	560	425	1400
Sp_1	408	421	0.92	1.5	730	NA	920
Sp_3	445	455	0.69	1.1	460	NA	710

[a] Vibrational frequencies obtained from analyzing emission bands in terms of Gaussian-shaped components. [b] Refers to excitation (λ = 620 nm) into the EXP unit. [c] Independent of excitation wavelength.

The isolated spacer groups are highly fluorescent in $CHCl_3$ and possess τ_S values in the region of 1 ns (Table 1). Fluorescence is structured and characterized by a relatively small Stokes' shift that decreases steadily with increasing molecular length. Likewise, the Huang−Rhys factor[57] falls progressively from 0.77 for Sp_0 to 0.63 for Sp_3. These latter findings indicate that the structural change upon excitation becomes smaller as the conjugation length increases,[58] probably because of the increased tendency to adopt a coplanar geometry in the ground state. For these compounds, k_{RAD} is relatively high and only weakly dependent on the molecular length. There have been

(57) (a) Markvart, T.; Greef, R. *Chem. Phys.* **2004**, *121*, 6401–6405. (b) Marletta, A.; Guimarães, F. E. G.; Faria, R. M. *Braz. J. Phys* **2002**, *32*, 570–574. (c) Lavrentiev, M. Y.; Barford, W. *J. Chem. Phys.* **1999**, *111*, 11177–11182.

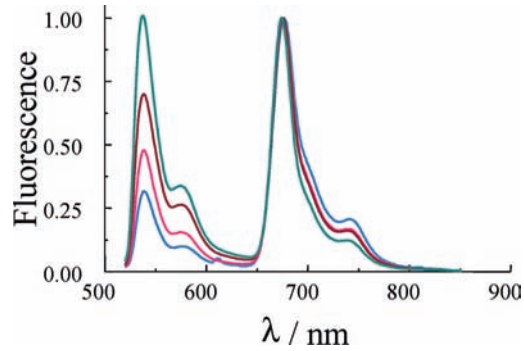

Figure 4. Fluorescence spectra recorded for the BOD_N−EXP triads in MTHF at 77 K following selective excitation into the BOD unit at 490 nm; BOD_0−EXP (light blue), BOD_1−EXP (red), BOD_2−EXP (brown) and BOD_3−EXP (green). Note that the spectra have been arbitrarily normalized at the emission peak for the EXP unit.

several prior investigations[59] into the photophysical properties of poly(aromatic) spacers of the type considered here, and a key factor concerns the level of electronic communication (v_N) between individual repeat units. This latter term can be evaluated[60] from absorption and emission spectral maxima (see Supporting Information) as being 6035 and 4400 cm^{-1}, respectively, for the Franck−Condon and relaxed S_1 states. It is important to stress that this level of electronic communication is sufficient for the spacer to function as a single chromophore as opposed to a chain of individual subunits. Thus, the spacer should be considered as one entity and not as an accretion of 1,4-phenylene-diethynylene units. Clearly, this feature is important when considering the fate of photons absorbed directly by the spacer.

Bridge-Mediated EET between the Terminals. Throughout the series of BOD_N−EXP triads in $CHCl_3$ at room temperature, fluorescence from the BOD unit could be observed following excitation at 490 nm, where EXP is transparent. A similar situation was found at 77 K in a MTHF glass (Figure 4). In each case, the measured Φ_F was reduced relative to that for the corresponding BOD_N dyad, and there was an analogous decrease in τ_S (see Supporting Information and Table 2). The derived Φ_F and τ_S values are clearly sensitive to the length of the spacer unit. Under the same conditions, there was sensitized fluorescence from the EXP unit, which decayed with the usual lifetime but for which time-resolved fluorescence decay profiles showed a distinct growth after the excitation pulse (Figure S1, Supporting Information). Such behavior is highly indicative of EET from BOD to EXP. Furthermore, these photophysical properties

Table 2. Summary of Properties Relating to Intramolecular EET from BOD to EXP As a Function of Spacer Length, Measured at Room Temperature in $CHCl_3$ Solution

cmpd	R_{BB}/Å	Φ_F [a]	τ_S/ns [a]	k_{EET} /10^9 s^{-1}	P_{EET}/% [b]	ΔE_{SS}/cm^{-1} [c]	λ_{SS}/cm^{-1} [d]
BOD_0−EXP	18	0.027	0.20	4.90	95	3670	620
BOD_1−EXP	24	0.100	0.52	1.70	88	3610	630
BOD_2−EXP	31	0.130	0.64	1.30	85	3575	665
BOD_3−EXP	38	0.175	0.71	1.15	80	3500	685

[a] Fluorescence quantum yield or lifetime of the S_1 state associated with the BOD unit. [b] Probability of EET in the triad as derived from excitation spectra. [c] S_1−S_1 energy gap. [d] Total reorganization energy accompanying EET.

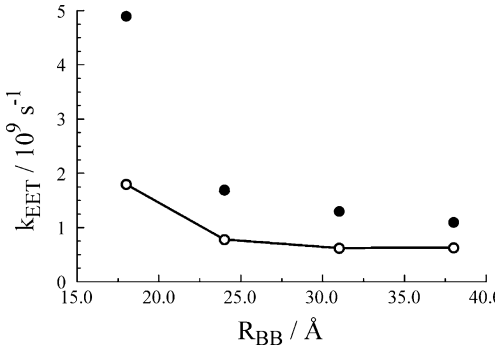

Figure 5. Effect of increasing molecular length on the rate constant for intramolecular EET in the BOD_N−EXP triads in $CHCl_3$ solution at room temperature (●) and in a MTHF glassy matrix at 77 K (○).

were found to be insensitive to changes in concentration, at least over a 15-fold range, such that intermolecular interactions can be ruled out. The probability (P_{EET}) of intramolecular EET was determined by critical comparison of the corrected excitation spectrum with the corresponding absorption spectrum (Table 2). Such spectral agreement decreases progressively with increasing spacer length. Likewise, the rate constant for intramolecular EET (k_{EET}), as determined from comparison of the fluorescence lifetimes of triad and dyad measured under identical conditions, decreases as the spacer becomes longer. The activation energy for intramolecular EET is only ~2 kJ mol^{-1} and remains insensitive to changes in the molecular length. It is also notable that both the S_1−S_1 energy gaps (ΔE_{SS}) and the total reorganization energies (λ_{SS}) accompanying EET, as derived from spectroscopic data, are only slightly affected by changes in the nature of the spacer unit (Table 2).

Figure 5 shows how k_{EET} evolves with increasing molecular length in $CHCl_3$ at room temperature and in a MTHF glassy matrix at 77 K. In both cases, there is a 4-fold decrease in rate constant on extending the B−B distance by 20 Å. Most of this decrease occurs between BOD_0 and BOD_1 and further increases in molecular length cause but a small decline in k_{EET}. The form of Figure 5 does not correspond to either the exponential falloff predicted by superexchange theory[21] or the inverse $(R_{BB})^6$ dependence required by Förster theory.[20] There are at least two cases reporting similar effects: Thus, Wasielewski et al. have described[61] a shallow, nonlinear dependence of the rate of electron transfer with donor−acceptor separation distance, which was interpreted in terms of a switch in mechanism from superexchange to hopping as the conjugated bridge became longer. This type of behavior seems unlikely for our system since the energy of the spacer always exceeds that of the donor

(58) (a) Liess, M.; Jeglinski, S.; Vardeny, Z. V.; Ozaki, M.; Yoshino, K.; Ding, Y.; Barton, T. *Phys. Rev. B* **1997**, *56*, 15712–15724. (b) Oliveira, F. A. C.; Cury, L. A.; Righi, A.; Moreira, R. L.; Guimaraes, P. S. S.; Matinaga, F. M.; Pimenta, M. A.; Nogueira, R. A. *J. Chem. Phys.* **2003**, *119*, 9777–9782. (c) O'Neill, L.; Byrne, H. J. *J. Phys. Chem. B* **2005**, *109*, 12685–12690. (d) Allen, B. D.; Benniston, A. C.; Harriman, A.; Llarena, I.; Sams, C. A. *J. Phys. Chem. A* **2007**, *111*, 2641–2649.

(59) (a) Mauthner, G.; Plank, H.; List, E. J. W.; Wenzl, F. P.; Bouguettaya, M.; Reynolds, J. R. *Phys. Rev. B* **2006**, *74*, 085208/1−085208/10. (b) Ebihara, Y.; Vacha, M. *J. Phys. Chem. B* **2008**, *112*, 12575–12578. (c) Di Paolo, R. E.; de Melo, J. S.; Pina, J.; Burrows, H. D.; Morgado, J.; Macanita, A. L. *ChemPhysChem* **2007**, *8*, 2657–2664. (d) Barbara, P. F.; Gesquiere, A. J.; Park, S. J.; Lee, Y. J. *Acc. Chem. Res.* **2005**, *38*, 602–610. (e) Monkman, A. P.; Burrows, H. D. *Synth. Met.* **2004**, *141*, 81–86.

(60) (a) Chang, R.; Hsu, J. H.; Fann, W. S.; Liang, K. K.; Chang, C. H.; Hayashi, M.; Yu, J.; Lin, S. H.; Chang, E. C.; Chung, K. R.; Chen, S. A. *Chem. Phys. Lett.* **2000**, *317*, 142–152. (b) Mirzov, O.; Scheblykin, I. G. *Phys. Chem. Chem. Phys.* **2006**, *8*, 5569–5576.

(61) Davis, W. B.; Ratner, M. A.; Wasielewski, M. R. *J. Am. Chem. Soc.* **2001**, *123*, 7877–7886.

Table 3. Parameters Derived in Connection with the Coupling Matrix Elements for Long-Range EET

cmpd	R_{BB}/Å [a]	V_{DA}/cm^{-1}	V_{COUL}/cm^{-1}	V_{BM}/cm^{-1}	ΔE_{DB}/cm^{-1}
BOD_0−EXP	18	1.52	0.21	1.31	7935
BOD_1−EXP	24	0.53	0.088	0.44	5540
BOD_2−EXP	31	0.40	0.040	0.36	4250
BOD_3−EXP	38	0.34	0.022	0.32	3500

[a] Refers to the distance between the two boron atoms as determined from the in vacuo PM3 energy-minimized structures obtained by computer modeling using TURBOMOLE.

and we have been unable to resolve an intermediate species other than the S_1 state localized on the BOD terminal. Separately, Albinsson et al. have described[62] systems where the rate of triplet EET depends on the energy gap between the donor and the spacer. Providing the dominant EET mechanism involves through-bond interactions, we might expect a comparable effect to hold for the systems examined herein. However, a not unreasonable explanation for the form of Figure 5 is that EET involves a combination of both through-space and through-bond mechanisms and, before looking deeper into the significance of the length dependence, this possibility needs to be resolved.

Now, the overall rate constant for EET can be expressed in terms of eq 1 where J_{DA} is the spectral overlap integral, which has an averaged value of 5.2×10^{-4} cm for the current BOD_N−EXP series, and V_{DA} is the overall matrix coupling element. As a consequence, the V_{DA} terms can be obtained from the measured k_{EET} values (Table 3). This latter term can be split into Coulombic (V_{COUL}) and bridged-mediated (V_{BM}) components according to eq 2. The matrix element for Coulombic interactions can be computed from spectroscopic properties as illustrated by eq 3, where s is a screening factor,[63] κ is the orientation factor,[64] R_{DA} is the distance between the centers of the relevant transition moment vectors, and d_D (or d_A) is the transition dipole moment[65] for the donor (or acceptor). The required parameters are readily available for the BODIPY-based dyes[66] and were used to calculate V_{COUL} for each system (Table 3). It can be seen that Coulombic interactions account for only a modest fraction of the overall EET mechanism and that bridge-mediated effects are dominant across all molecular lengths. From eq 4, we note that the matrix element for bridge-mediated coupling can be considered in terms of individual matrix elements for coupling between donor and bridge (V_{DB}) and between the acceptor and bridge (V_{AB}).[67] This particular term is modulated by the energy gap between donor and bridge (ΔE_{DB}); it should be stressed that superexchange theory is valid only when ΔE_{DB} exceeds υ_N by a factor of at least 5-fold.[68] These latter energy gaps can be obtained from spectroscopic data (see Supporting Information).

$$k_{EET} = \frac{2\pi}{\hbar}|V_{DA}|^2 J_{DA} \quad (1)$$

$$V_{DA}^2 = V_{COUL}^2 + V_{BM}^2 \quad (2)$$

$$V_{COUL} = s\kappa\frac{|d_D||d_A|}{R_{DA}^3} \quad (3)$$

$$V_{BM} = \sum_i \frac{V_{DB^i}V_{AB^i}}{\Delta E_{DB^i}} \quad (4)$$

Now, returning to the effect of the spacer length on k_{EET}, we can consider the bridge-mediated process separately from the Förster-type mechanism,[20] knowing that the latter accounts for no more than 15% of the total EET event. The derived coupling element (V_{BM}) evolves slowly with increasing molecular length and does not display an exponential dependence on R_{BB}. Correcting for changes[62] in ΔE_{DB} smoothes the curve somewhat but does not restore the exponential dependence, and it is clear that superexchange theory does not hold for this series of triads. Indeed, if we treat each spacer as being a single entity then there is no reason to suppose that V_{BM} should show a simple correlation with the molecular length. Perhaps the simplest alternative approach is to assume that k_{EET} at orbital contact takes on a value of $\sim 10^{12}$ s^{-1}, which on the basis of eq 1 corresponds to $V_{BM} \approx 40$ cm^{-1}. We can then express the length dependence in the form of eq 5 and assign to each spacer a characteristic resistance (Ω) that takes into account its particular length. Now, we see that the two shortest bridges (namely Sp_0 and Sp_1) share a common Ω value of 0.19 Å^{-1}, but the two longer spacers (namely, Sp_2 and Sp3) exhibit Ω values of 0.15 and 0.13 Å^{-1}, respectively. The differences in these Ω values are quite profound in view of the desire to transfer photons over relatively large distances, but it has to be recalled that the actual transfer probabilities (P_{EET}) fall off noticeably over the series. It is perhaps more significant to note an apparent correlation between the derived Ω value for a particular spacer and the experimental S factor derived from fitting[69] the emission spectrum of the isolated spacer unit. This is an intriguing observation in that it points to a facile way by which to predict the molecular resistance of a spacer unit without recourse to protracted synthesis.

$$V_{BM} = V_{BM}^0 e^{-\Omega R_{BB}} \quad (5)$$

Illumination into the Spacer Unit. It is difficult to resolve fluorescence emitted by the spacer from the baseline following UV excitation of the various BOD_N dyads in $CHCl_3$, despite the realization that the isolated spacers are highly emissive

(62) (a) Eng, M. P.; Albinsson, B. *Chem. Phys.* **2009**, *357*, 132–139. (b) Eng, M. P.; Martensson, J.; Albinsson, B. *Chem.—Eur. J.* **2008**, *14*, 2819–2826. (c) Eng, M. P.; Albinsson, B. *Angew. Chem., Int. Ed.* **2006**, *45*, 5626–5629. (d) Eng, M. P.; Ljungdahl, T.; Martensson, J.; Albinsson, B. *J. Phys. Chem. B* **2006**, *110*, 6487–9491.

(63) (a) Pojsl, M. *Czech. J. Phys.* **2000**, *50*, 1117–1124. (b) Andrews, D. L.; Juzeliunas, G. *J. Lumin.* **1994**, *60*, 834–837. (c) Hsu, C.-P.; Fleming, G. R.; Head-Gordon, M.; Head-Gordon, T. *J. Chem. Phys.* **2001**, *114*, 3065–3072.

(64) (a) Sani, S.; Singh, H.; Bagchi, B. *J. Chem. Sci.* **2006**, *118*, 23–35. (b) Wong, K. F.; Bagchi, B.; Rossky, P. J. *J. Phys. Chem. A* **2004**, *108*, 5725–5763.

(65) Alden, R. G.; Johnson, E.; Nagarajan, V.; Parson, W. W.; Law, C. J.; Cogdell, R. G. *J. Phys. Chem. B* **1997**, *101*, 4667–4680.

(66) (a) For both BOD and EXP, the transition dipole moment vectors are parallel to the long molecular axis. The center-to-center separation distances can be conveniently represented by the distances between the *meso*-carbon atoms in donor and acceptor. The computed orientation factors are small and probably underestimated by this point charge method. It has been shown, however, that reasonable estimates for the Coulombic coupling element can be obtained for related structures (see ref 66b), although the transition density cube method might be more appropriate (see ref 66c). (b) Ziessel, R.; Alamiry, M. A. H.; Elliott, K. J.; Harriman, A. *Angew. Chem., Int. Ed.* **2009**, *48*, 2772–2776. (c) Krueger, B. P.; Scholes, G. D.; Fleming, G. R. *J. Phys. Chem. B* **1998**, *102*, 5378–5386.

(67) Newton, M. D. *Int. J. Quantum Chem.* **2000**, *77*, 255–263.

(68) (a) McConnell, H. M. *J. Chem. Phys.* **1961**, *35*, 508–515. (b) Reimers, J. R.; Hush, N. S. *Chem. Phys.* **1989**, *134*, 323–354.

(69) Benniston, A. C.; Harriman, A.; Li, P. Y.; Sams, C. A. *J. Phys. Chem. A* **2005**, *109*, 2302–2309.

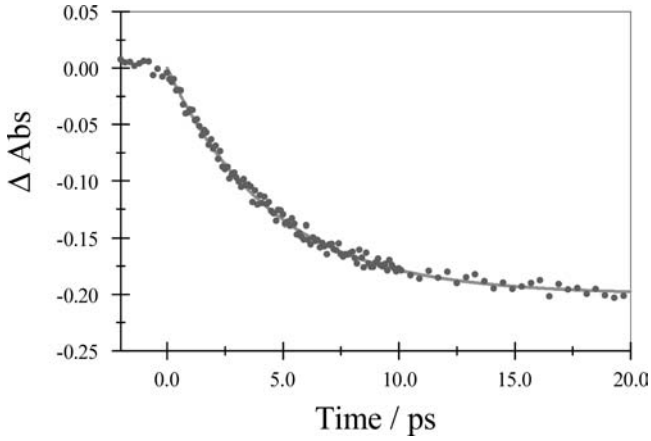

Figure 6. Transient bleaching signal observed for the BOD unit in BOD_1 following laser excitation into the spacer unit at 310 nm; $CHCl_3$ solution at room temperature.

Table 4. Parameters Associated with EET from the Spacer Unit, Measured in $CHCl_3$ at Room Temperature

cmpd	τ_S/ps	P_{BOD}/% [a]	P_{EXP}/% [a]	$J_{DA}(S_1)/10^4$ cm	$J_{DA}(S_2)/10^4$ cm
BOD_0	2.3	100	NA	7.3	42.6
BOD_1	4.5	100	NA	12.5	22.0
BOD_2	7.3	100	NA	18.3	6.3
BOD_3	11.5	100	NA	24.1	0.9
BOD-S_0−EXP [b]	1.6	65	35	0.06	27
BOD-S_1−EXP [b]	2.1	55	45	0.07	17
BOD_2−EXP [b]	4.2	45	55	0.09	9.5
BOD_3−EXP [b]	4.9	55	45	0.10	4.6

[a] Probability of EET to either BOD or EXP terminals, as determined from the excitation spectrum. [b] Entries for the overlap integrals refer to coupling between BOD and the EXP unit, while the individual entries refer to either the S_0-S_1 or S_0-S_2 absorption transitions localized on the EXP chromophore.

(Table 1). Under the same conditions, strong fluorescence is observed from the BODIPY-based dye and there is good agreement between the corrected excitation spectrum and the absorption spectrum across the near-UV region. As such, we can conclude that almost quantitative EET occurs from the spacer unit to the terminal BODIPY dye. The lifetime of the residual spacer-based fluorescence is too short ($\tau_S < 30$ ps) to be measured by our time-correlated, single-photon counting techniques. In contrast, the fluorescence lifetime of the BODIPY-based dye remained the same as that measured after direct excitation into the BODIPY dye (Table 1), while the decay profile showed no apparent grow-in after the excitation pulse (see Supporting Information). The rate constant for EET from spacer to dye could be measured by transient absorption spectroscopy after excitation at 310 nm, where the dye does not absorb appreciably compared to the spacer. A convenient experimental approach involves monitoring the onset of bleaching of the BODIPY-based absorption band at 528 nm. Indeed, transient bleaching could be described reasonably well as a single-exponential process (Figure 6), and such fitting allowed determination of the rise-times for population of the S_1 state localized on the BODIPY terminal (Table 4). There is a strong sensitivity toward the length of the spacer unit, although EET is fast in all cases, with the rate of EET decreasing steadily with increasing molecular length.

For BOD_0 there is essentially no spectral overlap ($J_{DA}(S_1)$) between spacer-based fluorescence and absorption by the S_1 state associated with the BODIPY dye (Table 4). This is not the case, however, for the S_0-S_2 absorption transition localized on the dye, where the overlap integral ($J_{DA}(S_2)$) is quite pronounced, and it is tempting to conclude that, for this system, EET will occur preferentially to the S_2 level of the acceptor. Such behavior has been reported previously for pyrene-based fluorophores appended to BODIPY.[41a,d] The opposite situation seems likely to hold for BOD_3 since overlap with the S_0-S_2 absorption transition is minimal but that with the S_0-S_1 transition is quite high (Table 4). The intermediate spacers could utilize both S_1 and S_2 states on the acceptor, and given the fact that the transition dipole vectors are essentially orthogonal, it seems most likely that EET occurs via electron exchange despite the unfavorable angle at the *meso*-position. It appears that the k_{EET} values (taken simply as the reciprocal of the singlet excited-state lifetime measured for the spacer) do not correlate particularly well with the total J_{DA} values. Instead, overlap with the S_2 state localized on the BOD acceptor seems to play the dominant role. This finding suggests to us that the corresponding coupling element for the S_2 state exceeds that for coupling to the S_1 state. Of course, there is every reason to suppose that the magnitudes of the coupling elements will vary along the series.

Similar studies were carried out with the analogous triads in $CHCl_3$, although it is not possible to avoid partial excitation into the BODIPY-based terminals. Here, illumination into the spacer unit gives rise to three distinct fluorescence bands, these being associated with spacer, BOD, and EXP (Figure S3, Supporting Information). It is interesting to note that, in each case, the ratio of fluorescence yields attributable to BOD and EXP differs from that obtained following direct excitation into the BOD terminal. This finding indicates that EET from the spacer unit does not selectively populate the excited-state manifold localized on BOD but leads to a distribution of excited states. By comparing the fluorescence spectral profiles recorded for each triad with the corresponding equimolar mixture of the appropriate reference compounds, it is possible to correct for the minor amount of direct absorption by the terminal. Subsequent comparison between fluorescence spectra recorded for the BOD_N dyads and BOD_N−EXP triads allows determination of the partitioning of the photon balance between BOD and EXP following excitation of the spacer. This situation is expressed in terms of the probability (P_B) of EET to each terminal (Table 4). It should be noted that EET from spacer to EXP must proceed via the S_2 state on the acceptor since the spectral overlap integral for the S_1 state is close to zero.

The outcome of this analysis is that for BOD_0−EXP, the internal EET distribution favors population of the BOD-based excited-state manifold. This can be traced to the more pronounced spectral overlap. Now, monitoring fluorescence associated with the EXP terminal shows that the S_1 state is formed in two distinct steps. The first crop arises within the excitation pulse, but the second step is much slower and clearly corresponds to EET from the BOD-based terminal (Figure 7). For the intermediate spacer lengths, BOD_1−EXP and BOD_2−EXP, partitioning of the internal EET process seems to scale with the relative $J_{DA}(S_2)$ values, overlap to the BOD-based S_1 state contributing little to the overall event. These values are similar for the two spacers but move in favor of the EXP terminal as the molecular length increases. For BOD_3−EXP, the distribution slightly favors the BOD-based terminal, and this is most likely a consequence of direct EET to the S_1 state.

Extending the Light-Harvesting Capability. One of the primary motivations for developing multichromophoric arrays of the type described herein relates to the design of improved

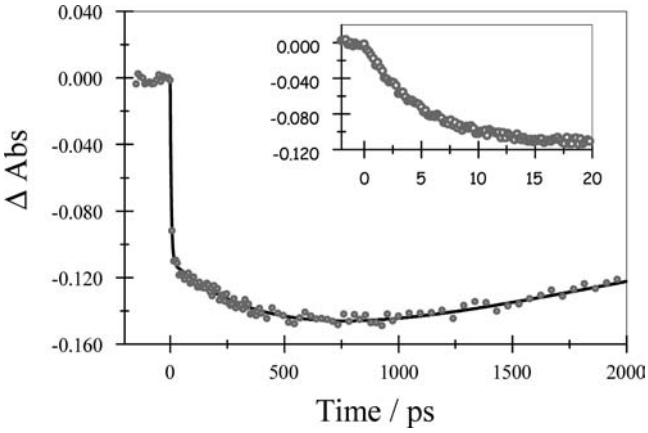

Figure 7. Transient bleaching signal observed for the EXP unit in BOD_1−EXP following laser excitation into the spacer unit at 310 nm, $CHCl_3$ solution at room temperature. The insert shows an expanded plot for the first 20 ps after the laser pulse.

solar concentrators.[45] The main function of such materials is to harvest photons across the visible region and transport the excitation energy to a site where chemical reactions can be initiated. The most effective solar concentrators comprise organic dyes[70] or silicon quantum dots,[71] dispersed in transparent plastic sheets, and these can be used to sensitize a range of solar cells, photoelectrochemical systems, and related light-driven devices.[72] Clearly, these BOD_N−EXP triads appear to be promising reagents for use as solar concentrators, and in order to improve their light-harvesting capability, further functionalization was undertaken. Specifically, the residual B−F bonds of the normal BODIPY chromophore were replaced with pyrene residues that absorb strongly in the near-UV region.[40c,45,73] The resultant molecular tetrad is illustrated in Scheme 2 and abbreviated as PY−BOD_0−EXP.

The absorption spectrum recorded for the tetrad in MTHF solution is shown in Figure 8 and displays clear features that can be attributed to the individual components, bearing in mind the number of appendages of each type. The EXP unit is well resolved in the red region (λ_{MAX} = 645 nm) of the visible range and remains essentially unperturbed with respect to the isolated chromophore. Likewise, absorption transitions localized on the BOD units are apparent at 522 nm and show no electronic perturbations imposed by the pyrene residues. These latter units exhibit a series of well-resolved absorption bands across the near-UV region, with the lowest-energy transition being located at 370 nm. Unfortunately, absorption transitions associated with the short spacer units are obscured by pyrene-based π,π^* bands but contribute to the absorption profile around 410 nm. The tetrad obeys the Beer−Lambert law over a modest concentration range and shows no obvious signs of aggregation under these

Scheme 2. Molecular Formula of the Pyrene-Substituted Tetrad

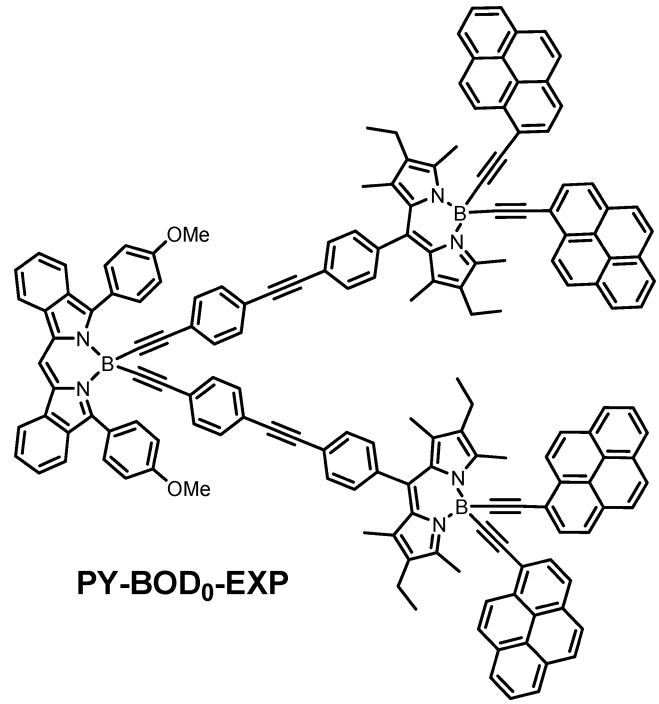

conditions. Furthermore, the compound can be dispersed in poly(methylmethacrylate) (PMMA) and cast into a thin film that shows very similar absorption spectral features. These films are stable over some considerable time when left under ambient light exposure.

Fluorescence from the EXP unit is observed readily around 672 nm following illumination into this chromophore at 600 nm (Figure 8). The fluorescence lifetime is 7.5 ns in $CHCl_3$ at room temperature, which remains comparable to those recorded for the triad series. On illumination into the BOD unit at around 495 nm, two fluorescence bands can be resolved. The lowest-energy emission is centered at about 670 nm and clearly corresponds to fluorescence from the EXP unit, while the higher-energy band is centered at ~537 nm and can be assigned to the BOD unit. For this latter emission, the fluorescence lifetime is 0.27 ns. This value is considerably shorter than that found for

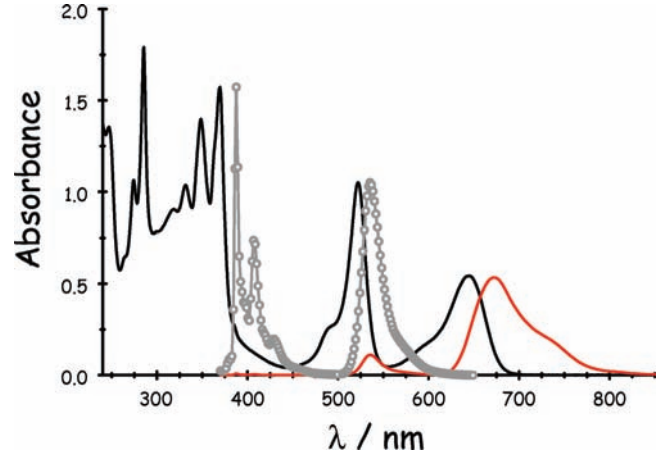

Figure 8. Absorption (black line) and fluorescence (red line) spectra recorded for PY−BOD_0−EXP in $CHCl_3$ at room temperature; the excitation wavelength for the emission spectrum was 360 nm. Also shown (in dotted gray curves) are expanded spectra of the pyrene- and BOD-based emission peaks.

(70) (a) El-Shahawy, M. A.; Mansour, A. F. *J. Mater. Sci.: Mater. Electron.* **1996**, *7*, 171–174. (b) Evenson, S. A.; Rawicz, A. H. *Appl. Opt.* **1995**, *34*, 7231–7238. (c) Kondepudi, R.; Srinivasan, S. *Ind. J. Pure Phys* **1990**, *28*, 334–337. (d) Koeppe, R.; Sariciffci, N. S.; Buchtemann, A. *Appl. Phys. Lett.* **2007**, *90*, 183516.
(71) (a) Chatten, A. J.; Burnham, K. W. J.; Buxton, B. F.; Ekins-Daukes, N. J.; Malik, M. A. *Semiconductors* **2004**, *38*, 909–917. (b) Gallagher, S. J.; Norton, B.; Eames, P. C. *Sol. Energy* **2007**, *81*, 813–821. (c) Reda, S. M. *Acta Mater.* **2008**, *56*, 259–264.
(72) (a) Gombert, A.; Luque, A. *Phys. Status Solidi A* **2008**, *205*, 2757–2765. (b) Franco, J.; Saravia, L.; Javi, V.; Caso, R.; Fernandez, C. *Solar Ener.* **2008**, *82*, 1088–1084. (c) Lambert, M. A. *Appl. Therm. Eng.* **2007**, *27*, 1612–1628.
(73) Bonardi, L.; Ulrich, G.; Ziessel, R. *Org. Lett.* **2008**, *10*, 2183–2186.

the reference compound, BOD_0 ($\tau_S = 5.4$ ns) but longer than that observed for the corresponding triad, BOD_0−EXP ($\tau_S = 0.20$ ns). The decreased lifetime relative to BOD_0 can be attributed to EET from BOD to EXP, for which the rate constant k_{EET} is calculated as being 3.5×10^9 s^{-1}. This derived k_{EET} is slightly smaller than that found for BOD_0−EXP ($k_{EET} = 4.9 \times 10^9$ s^{-1}), thereby suggesting that the appended pyrene units have an effect on the geometry or electronic properties of the system, as previously observed by electrochemical experiments on PY−BOD analogues.[47] This is a fairly modest change in rate constant, however, and the transfer probability ($P_{EET} = 95\%$) remains high for the tetrad. It should be noted that the concept of intramolecular EET was fully supported by the close agreement between absorption and excitation spectra. Similar effects were noted for PY−BOD_0−EXP dispersed in PMMA.

Illumination into the pyrene units present in the tetrad gave rise to extremely weak emission characteristic of that chromophore, this being centered at ~404 nm (Figure 8), but the lifetime was too short to be resolved by time-correlated, single-photon counting methods ($\tau_S < 30$ ps) in $CHCl_3$ solution. Excitation spectra recorded for emission from both BOD and EXP units confirmed that efficient EET from pyrene occurs, although logically EET takes place exclusively to the nearby BOD unit and is subsequently transferred to the terminal EXP acceptor. Comparison with 1-ethynylpyrene[74] allows estimation of k_{EET} for this process as being $>3 \times 10^{10}$ s^{-1}, while P_{EET} exceeds 98% under these conditions. Very efficient EET has been reported for other pyrene−Bodipy dyads[41a,d] and attributed to a combination of through-space and through-bond mechanisms. Indeed, the present case seems to be in good accord with prior systems. The short linker favors rapid EET, which involves primarily the S_2 state on the Bodipy acceptor for which the spectral overlap integral is calculated to be 0.0012 cm. It is also important to note that 1-ethynylpyrene[74] is highly fluorescent ($\Phi_F = 0.8$) and possesses a relatively long-lived excited state ($\tau_S = 13$ ns).

A consequence of the highly efficient EET from PY to BOD in the tetrad is that there is no need to consider competing intramolecular EET steps between PY units. However, this might not be the case for energy migration between BOD units, where a through-space mechanism could operate. It is, however, a straightforward matter to compute Förster-type rate constants for energy migration (k_{EM}) for the various triads, restricting attention solely to the dye units. The result is that the Förster critical distance (R_0) is estimated to be ~29.5 Å for random orientations of EXP units. The same calculation carried out for the isolated BOD units places R_0 at ~20.0 Å; this falls to 13.5 Å for BOD_0−EXP because of the competing intramolecular EET process. These R_0 values are outside the average separations expected for dilute solutions but are more relevant for solid matrices. Thus, with a low loading of PY−BOD_0−EXP in PMMA, weak (i.e., <2% of the total emission) fluorescence is observed from PY, stronger (i.e., 10% of the total emission) fluorescence is apparent for the BOD unit and intense (i.e., 88% of the total emission) fluorescence appears from the EXP unit. Progressive increase of the loading leads to a decrease in fluorescence from both PY and BOD units but an increase in fluorescence from EXP (Figure S4). At high loadings, more than 99% of the total emission can be traced to the EXP unit which retains a fluorescence lifetime of 7.5 ns under these conditions. The increased P_{EET} is clearly a consequence of intermolecular steps augmenting the already efficient intramolecular processes. These bimolecular events could involve both energy migration among identical chromophores (e.g., BOD to BOD) or EET from (say) BOD to EXP (where $R_0 = 41$ Å).

The highest loading of PY−BOD_0−EXP in PMMA (film thickness 100 μm) achievable without special conditions corresponds to an average (i.e., nonrandom distribution) distance of ~35 Å. This value is comparable to the calculated critical distances, and is of the same order as the molecular length. As such, individual molecules will be in very close proximity within the anisotropic medium. This will facilitate intermolecular EET, as observed experimentally, and also promote energy migration between EXP units. At present, coherent energy migration might be expected over many hundreds of ångstroms, which is ideal for a sensitizer but might still be too short for an effective solar concentrator.

Concluding Remarks

It has been shown that EET between the terminals of the various molecular triads occurs primarily by way of through-bond, electron-exchange interactions, despite the orthogonal connection at the *meso*-site and the incorporation of a boron atom into the distal linkage. This conclusion is valid across all the available molecular lengths. That the actual coupling element for bridge-mediated EET shows a nonexponential dependence on the distance between the reactants is easily explained in terms of the evolving energy gap between donor and spacer. Furthermore, the basic conditions for superexchange interactions are not fulfilled inasmuch as the level of electronic communication between the repeat units in the bridge exceeds the donor−spacer energy gap in most cases, and even for the shortest spacer the two terms are comparable. A more surprising outcome, and one that is potentially of intense value, is the realization that the effective resistivity of the spacer with respect to long-range electron exchange can be related to its optical properties. Since the latter are easily measured, it follows that the effective resistance can be predicted without the need for elaborate synthesis or protracted photophysical investigation. The two main optical properties that evolve along the oligomeric series are the Stokes' shift (SS) and the Huang−Rhys factor. It is notable that both terms refer to structural changes that occur on illumination, and since the level of molecular conductance (or resistance) should also depend on the geometry of the spacer, we can see how the correlation arises.

The key factors associated with effective photon propagation along the spacer unit are the level of electronic communication between adjacent subunits and the ensuing geometry change on illumination. Both parameters depend on the molecular structure, being system dependent, but the latter term, which is exemplified by the Huang−Rhys factor, also varies with the spacer length. In fact, the Huang−Rhys factor should increase with increasing temperature due to an increase in the extent of disorder.[75] This latter effect could help explain the small activation energies observed for long-range EET. The fact that υ_N can change markedly for different electronic states, including the triplet-excited state,[54] confirms the notion that the molecular resistance of a short spacer depends on the actual system under investigation and is not simply a spacer-sensitive property. In the present case, the distance over which EET remains effective is set by the excited-state lifetime of the donor.

(74) (a) Pomestchenko, I. E.; Luman, C. R.; Hissler, M.; Ziessel, R.; Castellano, F. N. *Inorg. Chem.* **2003**, *42*, 1394–1396. (b) Benniston, A. C.; Harriman, A.; Howell, S. L.; Sams, C. A.; Zhi, Y. G. *Chem.—Eur. J.* **2007**, *13*, 4665–4674.

A singlet excited-state generated on the spacer module can undergo EET events with either of the terminals. In the case of the EXP-based terminal, the only significant spectral overlap occurs with the S_2 state on the acceptor, and the corresponding $J_{DA}(S_2)$ term decreases steadily with increasing spacer length. For the BOD-based terminal, spectral overlap occurs with both S_1 and S_2 states since emission from the spacer falls within the wavelength range between these two states. Overlap shifts progressively in favor of the S_1 state as the spacer becomes longer. Comparing the distribution patterns as a function of molecular length, and taking due account of the k_{EET} values found for the BOD_N dyads, leads to the conclusion that coupling to the S_2 level of the acceptor outweighs that to the S_1 state. This is a surprising result, but not much is known about the S_2 level of BODIPY-based dyes.[76] There does not seem to be a real preference for EET to either terminal, the distribution being set by the respective J_{DA} values, despite the fact that several overlapping transition are evident in the near-UV region for EXP, whereas the S_0-S_2 transition for BOD looks to be better resolved. Earlier work[76] has reported that internal conversion between S_2 and S_1 states is very fast (i.e., 100−250 fs) for conventional BODIPY-based dyes, but based on the new results generated here, it might be important to characterize these S_2 states in more detail.

Finally, we draw attention to the realization that PY−BOD_0−EXP reflects the main features that are of current concern with regards to the mechanism of long-range energy migration in conducting polymers. In such systems, a key aspect of the overall performance relates to distinguishing between intra- and interchain EET steps. It is clear from this work, and from other studies,[66b] that Förster theory cannot be relied on to compute accurate rates of EET for closely spaced reagents[77] or where the transition dipole vector is extended.[78] Detailed studies are needed to clarify how best to amend the Coulombic theory to account for such cases.

Acknowledgment. We thank the EPSRC (EP/D032946/1), Newcastle University, the Centre National de la Recherche Scientifique (CNRS), and the Ministère de la Recherche et de l'Education Nationale for financial support of this work.

Supporting Information Available: Full experimental details, including synthesis of all relevant compounds, and examples of NMR and emission spectra recorded under different conditions. This material is available free of charge via the Internet at: http://pubs.acs.org.

JA9038856

(75) (a) da Silva, M. A. T.; Dias, I. F. L.; Duarte, J. L.; Laureto, E.; Silvestre, I.; Cury, L. A.; Guimaraes, P. S. S. *J. Chem. Phys.* **2008**, *128*, 094902/1−094902/8. (b) Spano, F. C.; Silvestri, L.; Spearman, P.; Raimondo, L.; Tavazzi, S. *J. Chem. Phys.* **2007**, *127*, 184703/1–184703/12. (c) Winokur, M. J.; Slinker, J.; Huber, D. L. *Phys. Rev. B* **2003**, *67*, 184106/1–184106/11. (d) Schutze, J.; Bruggemann, B.; Renger, T.; May, V. *Chem. Phys.* **2002**, *275*, 333–354. (e) Harriman, A.; Rostron, S. A.; Khatyr, A.; Ziessel, R. *Faraday Disc.* **2006**, *131*, 377–391.

(76) Toele, P.; Zhang, H.; Trieflinger, C.; Daub, J.; Glasbeek, M. *Chem. Phys. Lett.* **2003**, *368*, 66–75.

(77) Curutchet, C.; Mennucci, B.; Scholes, G. D.; Beljonne, D. *J. Phys. Chem. B* **2008**, *112*, 3759–3766.

(78) Wong, K. F.; Bagchi, B.; Rossky, P. J. *J. Phys. Chem. A* **2004**, *108*, 5752–5763.